University of Sistan and Baluchestan

Chemical Process Design

Available online at http://cpd.usb.ac.ir/



Deep Eutectic Solvent-Assisted Preparation of Cellulose Nanoparticles from Peanut Shell Waste

Targol Najjaran Tousi[1], Zahra Hejri[2]✉, Maryam Omidvar[3], Nadia Sahebjamee[4]

[1] Department Of Chemical Engineering, Qu. C., Islamic Azad University, Quchan, Iran. Email: targolnt@gmail.com
[2] Corresponding Author, Department Of Chemical Engineering, Qu. C., Islamic Azad University, Quchan, Iran. Email: za.hejri@iau.ac.ir
[3] Department Of Chemical Engineering, Qu. C., Islamic Azad University, Quchan, Iran. Email: maryam.omidvar@iau.ac.ir
[4] Department Of Chemical Engineering, Qu. C., Islamic Azad University, Quchan, Iran. Email: sahebjamee@iau.ac.ir

ARTICLE INFO

Article type:
Research Article

Article history:
Received: 2026-08-01
Received in revised form: 2026-09-27
Accepted: 2026-09-29
Available online: 2026-09-29

Keywords: *Peanut shell; Deep eutectic solvent (DES); Cellulose; Nanoparticles*

ABSTRACT

This study presents an environmentally friendly method for extracting cellulose from peanut shells—an abundant agricultural by-product—and converting it into cellulose nanoparticles (CNPs). Cellulose was extracted using a choline chloride: urea (2:1) deep eutectic solvent (DES) at 90 °C for 3 h, followed by bleaching and subsequent mechanical disintegration using probe ultrasonication. The extracted cellulose and CNPs were characterized using Fourier-transform infrared spectroscopy (FTIR), X-ray diffraction (XRD), field-emission scanning electron microscopy (FE-SEM), transmission electron microscopy (TEM), dynamic light scattering (DLS), and zeta-potential analysis. FT-IR confirmed the substantial removal of non-cellulosic components while preserving cellulose integrity, whereas XRD indicated the retention of the cellulose structure with good crystallinity. FE-SEM and TEM revealed the formation of nanoscale cellulose structures with particle-like morphology. DLS provided quantitative information on the hydrodynamic size distribution and aggregation behavior of CNPs in aqueous suspension, while zeta-potential measurements indicated the colloidal stability of the resulting suspension. Overall, the results demonstrate that the choline chloride: urea DES provides a sustainable alternative to conventional alkaline–acid processes, avoiding hazardous chemicals while enabling the production of cellulose nanoparticles from peanut shell biomass. The produced CNPs show potential for applications in sustainable packaging, nanocomposites, and other cellulose-based functional materials

Cite this article: Najjaran Tousi, T., Hejri, Z., Omidvar, M., Sahebjamee, N., (2027), Deep Eutectic Solvent-Assisted Preparation of Cellulose Nanoparticles from Peanut Shell Waste, *Chemical Process Design*, 6(1), 1-14. http//doi.org/10.22111/cpd.2026.56492.1100

© The Author(s).
Publisher: University of Sistan and Baluchestan.
DOI: http//doi.org/10.22111/cpd.2026.56492.1100

ARTICLE IN PRESS

1. Introduction

Environmental pollution caused by non-degradable synthetic polymers has become a major global concern over the past decades [1]. This has stimulated intensive research on biodegradable and renewable materials for applications in

packaging, pharmaceuticals, food, and biomedical sectors [2]. Among natural biopolymers, cellulose and its derivatives are particularly attractive owing to their abundance, renewability, biocompatibility, and inherent biodegradability, alongside low cost and favorable mechanical properties [3].

Cellulose nanofibers (CNPs) have emerged as a key class of nanocellulose materials due to their high aspect ratio, excellent tensile strength and stiffness, low coefficient of thermal expansion, large specific surface area, and strong reinforcing capability in composite matrices [4,5]. These features make CNPs promising candidates for advanced applications such as polymer nanocomposites, sustainable packaging and barrier films, flexible substrates, and biomedical scaffolds [6].

While wood remains the dominant industrial source of cellulose, lignocellulosic agricultural residues provide low-cost, underutilized alternatives that align with circular economy concepts [7]. Common examples include cotton stalks, wheat straw, sugarcane bagasse, and peanut shells [8]. Peanut (Arachis hypogaea) is one of the most widely cultivated oilseed crops worldwide, with annual production exceeding 50 million metric tons in recent years [9]. Approximately 22–30% of the total mass corresponds to shells (hulls), resulting in more than 10–15 million metric tons of peanut shell waste annually [9]. This residue is often burned, landfilled, or used as low-value animal feed, contributing to environmental burdens and representing a missed opportunity for value-added utilization [10][9].

Peanut shells are a typical lignocellulosic biomass, mainly composed of cellulose (≈34–48%), hemicellulose (≈3–19%), and lignin (≈25–33%), depending on cultivar and processing conditions [11]. Their relatively high cellulose content, combined with wide availability and negligible economic value, makes peanut shells an attractive feedstock for the production of cellulose and nanocellulose-based materials [12,13]. However, effective utilization requires selective removal of lignin and hemicellulose while preserving the structural integrity of cellulose.

Conventional cellulose extraction routes from lignocellulosic biomass generally rely on alkaline pulping followed by acid hydrolysis (e.g., mineral acids) to isolate cellulose and generate nanofibers or nanocrystals [14,15]. Although these processes are effective, they suffer from significant drawbacks, including high consumption of corrosive chemicals, large effluent volumes, limited chemical recovery, equipment corrosion, and partial degradation or depolymerization of cellulose chains [16]. These issues raise environmental and economic concerns and motivate the development of greener, less hazardous pretreatment strategies.

In this context, deep eutectic solvents (DESs) have gained considerable attention as promising green media for biomass fractionation and pretreatment [17,18]. DESs are typically formed by mixing a hydrogen bond acceptor (choline chloride) with a hydrogen bond donor (e.g., urea, organic acids, or polyols) at specific molar ratios to obtain a liquid with a melting point lower than that of the individual components [19]. Compared with conventional organic solvents and even ionic liquids, DESs offer several advantages, such as low volatility, relatively low toxicity, simple and low-cost preparation, potential biodegradability, and tunable solvating power toward lignin and hemicellulose while maintaining cellulose integrity [18,20]. Recent studies have shown that DES-based pretreatments can achieve effective delignification under milder conditions, lower energy demand, and enable partial solvent recycling, thus supporting sustainable biorefinery concepts [18,21].

Despite growing interest in DES-assisted processing of lignocellulosic biomass, there are still relatively few reports focusing on peanut shells as a precursor for nanocellulose production using simple, low-toxicity DES systems. In particular, comprehensive studies that integrate DES pretreatment, subsequent mechanical disintegration, and multi-technique characterization (FE-SEM, TEM, FT-IR, XRD, DLS) of the resulting cellulose nanoparticles from peanut

ARTICLE IN PRESS

shells remain limited in the literature [22]. Therefore, the present study aims to develop and evaluate a sustainable, acid-free process for producing cellulose nanoparticles from peanut shells using a choline chloride :urea-based deep eutectic solvent as the pretreatment medium.

Although DES-based pretreatment has been increasingly investigated for the fractionation of lignocellulosic biomass, most reported nanocellulose production routes still rely on subsequent chemical hydrolysis, alkaline treatment, oxidation, or combinations of these processes to achieve nanoscale fibrillation. In this context, the novelty of the present study lies in integrating choline chloride :urea DES pretreatment of peanut shell biomass with subsequent probe-ultrasonication-assisted mechanical defibrillation, without employing acid hydrolysis or other chemical hydrolytic agents during nanoparticle formation. This integrated strategy aims to simplify the conversion pathway while preserving the native cellulose I structure and generating cellulose nanoparticle structures. The process was further evaluated through complementary FT-IR, FE-SEM, TEM, DLS, XRD, and zeta-potential analyses, providing a comprehensive assessment of chemical purification, morphological evolution, crystallinity, particle-size behavior, and colloidal stability.

2. Materials & Methods

2.1. Materials

Choline chloride (purity: 98%), urea (purity: 98%), hydrogen peroxide (H_2O_2, purity: 35%), acetone (purity: 99%), and potassium bromide (KBr, purity: 98%) were procured from Merck (Darmstadt, Germany). All chemicals were of analytical grade and used without any further purification unless otherwise specified. Potassium bromide was utilized for the preparation of FT-IR pellets during Fourier-transform infrared spectroscopy analysis. Deionized water was employed throughout the entire experimental process for solution preparation, washing, and all subsequent treatment steps.

Table 1. Materials and Chemicals Used in This Study

Material (Chemical)	Purity / Specification	Supplier	Role / Use
Peanut shells	Agricultural waste	Local sources	Raw lignocellulosic biomass
Choline chloride	98%	Merck (Darmstadt, Germany)	Hydrogen bond acceptor for DES preparation
Urea	98%	Merck (Darmstadt, Germany)	Hydrogen bond donor for DES preparation
Hydrogen peroxide (H_2O_2)	35%	Merck (Darmstadt, Germany)	Bleaching agent
Acetone	99%	Merck (Darmstadt, Germany)	Washing solvent
Potassium bromide (KBr)	98%	Merck (Darmstadt, Germany)	FT-IR pellet preparation
Deionized water	—	—	Solvent, washing, and suspension medium

2.2. Methods

2.2.1. Preparation of Peanut Shell Powder

Peanut shells were collected from local agricultural sources and thoroughly washed with deionized water to remove soil, dust, and other impurities. The cleaned shells were air-dried at room temperature for 24 hours and then stored in

ARTICLE IN PRESS

a cool and dry place. The dried shells were ground using a laboratory mill (e.g., IKA A11 basic analytical mill) and sieved through a 100-mesh screen to obtain uniform particle size (<150 μm). The resulting powder was dried in a preheated oven at 103°C and stored in a desiccator until use.

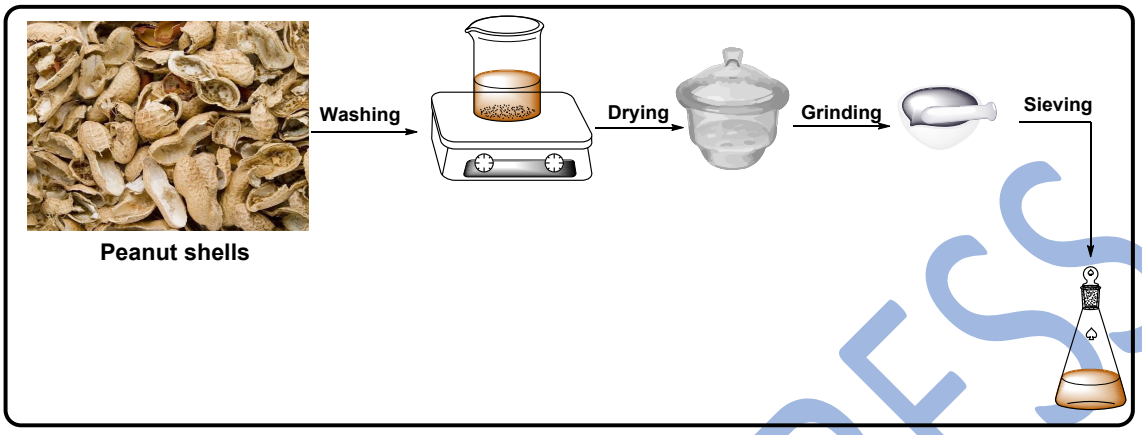


Fig 1. Preparation of peanut shell powder as a lignocellulosic feedstock for cellulose extraction. The raw peanut shells were washed, dried, ground, sieved, and stored under controlled conditions prior to the deep eutectic solvent (DES) pretreatment

2.2.2. Preparation of the Deep Eutectic Solvent (DES)

The DES was prepared by mixing choline chloride and urea in a 2:1 molar ratio. The mixture was heated to 80°C on a magnetic stirrer hot plate (IKA RH basic) with continuous stirring at 300 rpm for 15 minutes until a clear, homogeneous liquid formed. After cooling to room temperature, the prepared DES was transferred to a sealed glass container and stored in a desiccator to minimize moisture uptake

2.2.3. Cellulose Extraction

Peanut shell powder (1 g) was mixed with 20 mL of the prepared DES in a glass flask. The reaction mixture was stirred at 90 °C for 3 h at 500 rpm. Upon completion, it was cooled in an ice bath for 10 min and subsequently washed three times with 25 mL of a 1:1 (V/V) acetone–water solution to remove residual lignin and hemicellulose. Hydrogen peroxide (30% W/V, 5 mL) was then added to bleach residual impurities, and the suspension was stirred for an additional 30 minutes at room temperature. The product was filtered using a Büchner funnel with Whatman filter paper (grade 1), rinsed five times with 20 mL deionized water until neutral pH, and dried in a vacuum oven at 40°C for 12 hours.

2.2.4. Experimental Factors and Levels

To investigate the effect of processing conditions on cellulose nanoparticle production, three process parameters were considered during the nanoparticle formation stage suspension time, sonication time, and hydration time. Suspension time was investigated at four levels (0.5, 1, 2, and 3 h), sonication time at three levels (2, 3, and 4 h), and hydration time at two levels (6 and 12 h). Nanocellulose yield was selected as the primary response for evaluating the effect of these processing conditions.

The selected factors were based on their expected influence on the accessibility, dispersion, and mechanical disintegration of the extracted cellulose. Suspension and hydration times were considered because sufficient wetting and hydration of cellulose fibers can facilitate their dispersion and subsequent exposure to ultrasonic cavitation. Sonication time was selected as a key mechanical processing parameter because increasing exposure to ultrasonic cavitation can promote structural disintegration and the formation of nanoscale cellulose particles, while

ARTICLE IN PRESS

unnecessarily prolonged sonication may increase energy consumption and affect the dispersion state of the resulting nanoparticles.

The investigated ranges were selected to provide practical low-to-high processing conditions while avoiding unnecessarily prolonged treatment. The experimental combinations and corresponding nanocellulose yields are presented in Table 3.

Table 2. Experimental factors and levels investigated during cellulose nanoparticle production

Type	Parameter	Levels / measurement
Factor 1	Suspension time	0.5, 1, 2, 3 h
Factor 2	Sonication time	2, 3, 4 h
Factor 3	Hydration time	6, 12 h
Response	CNP yield	%

2.2.5. Preparation of Cellulose Nanoparticles (CNPs)

Extracted cellulose (0.32 g) was dispersed for 1h in 80 mL deionized water to form a 0.4% (W/V) suspension and stored at 4°C overnight to ensure hydration. The suspension was subjected to ultrasonication using a probe sonicator (Qsonica Q500) at 300 W power with a cycle of 3 seconds on and 7 seconds off for a total of 3 hours. To prevent overheating, the sample container was immersed in an ice-water bath. The sonicated suspension was centrifuged at 4500 rpm for 30 minutes (using a Sigma 3-16L centrifuge), the supernatant was discarded, and the pellet was resuspended in 20 mL deionized water. The final suspension was frozen at -80°C for 48 hours and then freeze-dried using a lyophilizer (Labconco FreeZone) at -50°C and 0.05 mbar for 24 hours to obtain dry CNPs.

ARTICLE IN PRESS

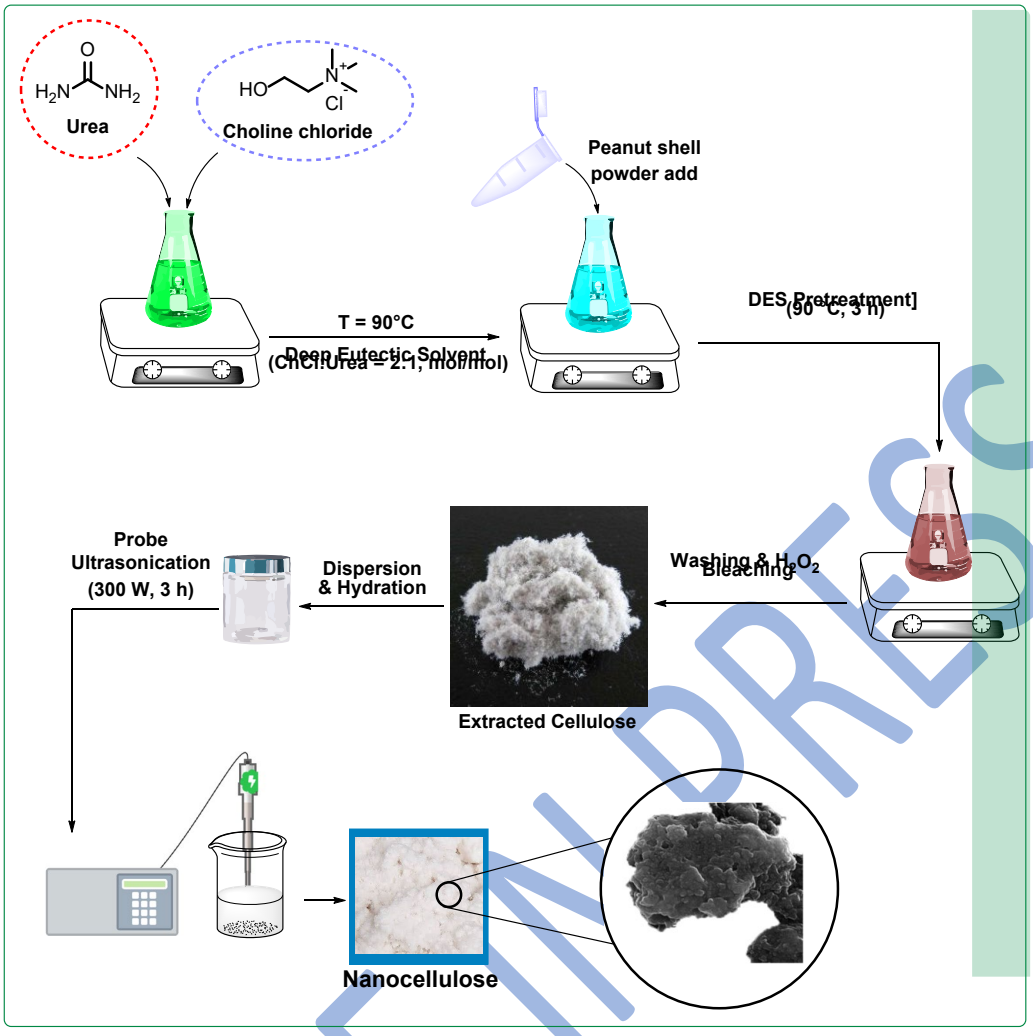


Fig 2. Schematic workflow for the sustainable production of nanocellulose from peanut shell biomass. Cellulose was extracted using a choline chloride/urea deep eutectic solvent (DES, 2:1 molar ratio) at 90 °C, followed by bleaching and purification with hydrogen peroxide, distilled water, and acetone. The purified cellulose was subsequently dispersed in water and converted into nanocellulose using probe ultrasonication (300 W, 3 h)

ARTICLE IN PRESS

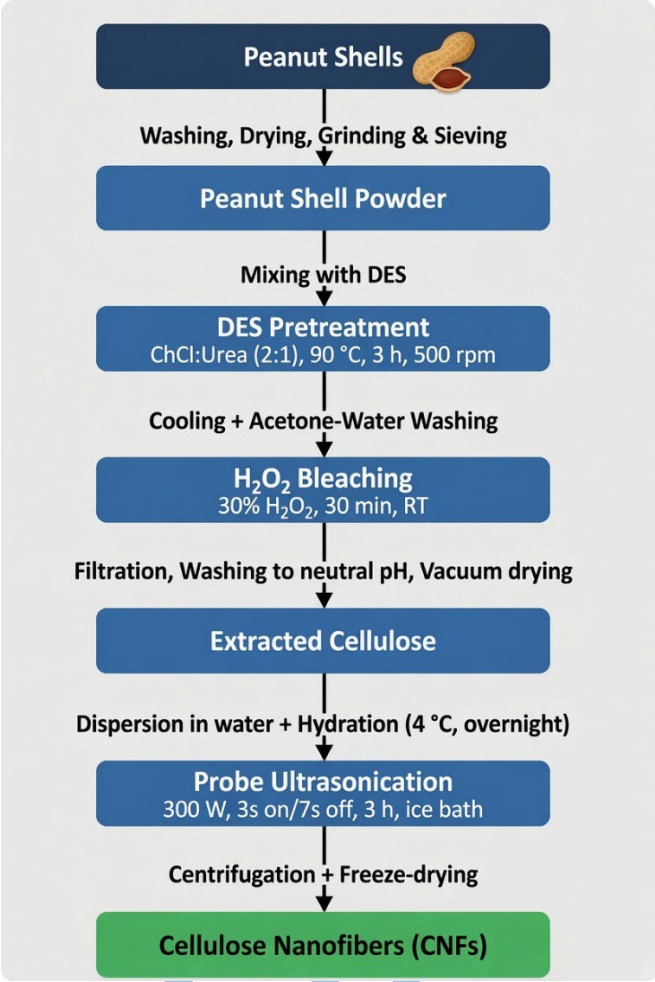


Fig 3. Schematic flowchart illustrating the complete process for the production of cellulose nanoparticles (CNPs) from peanut shell waste. The process includes powder preparation, deep eutectic solvent (DES) pretreatment using choline chloride : urea (2:1 molar ratio) at 90 °C for 3 h, hydrogen peroxide bleaching, dispersion and hydration of the extracted cellulose, probe ultrasonication (300 W, 3 h), and final freeze-drying to obtain CNPs

2.2.6. Yield of Cellulose Extraction and Cellulose Nanoparticle Production

The extraction yield and mass preservation efficiency of cellulose and nanocellulose are critical parameters for evaluating the technical feasibility, sustainability, and industrial applicability of biomass valorization processes. In the present study, the efficiency of the deep eutectic solvent (DES)-assisted extraction route was quantitatively assessed by calculating the cellulose extraction yield, CNP conversion yield, and the overall process yield from raw peanut shell biomass to the final nanocellulose product.

The cellulose extraction yield was determined according to Eq. (1).

$$Cellulose\ yield\ (\%) = \frac{W_c}{W_{ps}} \times 100 \quad (1)$$

where (W_c) is the dry weight of extracted cellulose and (W_{ps}) is the initial dry weight of peanut shell biomass.

Based on the experimental measurements, approximately 0.5 g of purified cellulose was obtained from 1.0 g of oven-dried peanut shell powder, corresponding to a cellulose extraction yield of approximately 50%. This relatively high yield demonstrates the remarkable efficiency of the DES pretreatment system in selectively removing lignin, hemicellulose, pigments, waxes, and other amorphous constituents while preserving a substantial fraction of the cellulose framework. Considering that peanut shells typically contain approximately 35–45 wt% cellulose in their native lignocellulosic composition, the obtained extraction yield indicates that the DES system achieved near-

complete recovery of the accessible cellulose fraction with minimal cellulose degradation or mass loss during processing.

The conversion yield of cellulose into nanocellulose was calculated using Eq. (2).

$$Nano\ cellulose\ (\%) = \frac{W_{nc}}{W_c} \times 100 \quad (2)$$

where (W_{nc}) represents the dry weight of the produced nanocellulose and (w_c) is the dry weight of purified cellulose subjected to ultrasonic defibrillation.

Experimentally, 0.4 g of nanocellulose was obtained from 0.5 g of purified cellulose, resulting in a CNP conversion yield of approximately 80%. Such a high conversion efficiency strongly suggests that the employed ultrasonication-assisted defibrillation strategy effectively disintegrated the cellulose microfibers into nanoscale structures while preserving the majority of the cellulose mass. This behavior is particularly significant because many conventional acid hydrolysis approaches often lead to excessive cellulose depolymerization, dissolution of amorphous and partially crystalline domains, and substantial material losses during repeated washing and centrifugation steps.

To further evaluate the overall efficiency of the integrated process, the total conversion yield from raw peanut shell biomass to nanocellulose was calculated using Eq. (3).

$$Overall\ yield\ (\%) = \frac{W_{nc}}{W_{ps}} \times 100 \quad (3)$$

The overall process yield was therefore determined to be approximately 40%, indicating that nearly half of the original lignocellulosic biomass was successfully transformed into value-added nanocellulose material. This result highlights the high biomass utilization efficiency of the DES-assisted route and demonstrates its strong potential as a sustainable strategy for agricultural waste valorization. The high extraction and conversion yields obtained in this study can be attributed to several synergistic effects associated with the choline chloride : urea DES system. First, the DES selectively disrupted hydrogen-bonding interactions within the lignin–hemicellulose matrix while minimizing disruption of the crystalline cellulose regions. Second, the relatively mild processing conditions reduced cellulose chain scission and prevented excessive degradation typically associated with concentrated mineral acids. Third, the DES environment likely enhanced swelling and accessibility of the biomass structure, facilitating efficient penetration of the solvent system and subsequent fibrillation during nanocellulose production. Importantly, the obtained yield values compare favorably with previously reported studies on peanut shell-derived cellulose and nanocellulose. Earlier investigations employing sulfuric acid hydrolysis, alkaline extraction, or TEMPO-mediated oxidation generally reported cellulose extraction yields in the range of approximately 25–40%, depending on treatment severity and purification conditions. Similarly, CNP conversion yields commonly decrease significantly under harsh acidic conditions due to cellulose degradation and material loss during purification. In contrast, the present DES-assisted strategy achieved both high cellulose recovery (50%) and high nanocellulose conversion efficiency (80%), while simultaneously preserving the cellulose crystalline structure, as confirmed by FT-IR, XRD, FE-SEM and TEM analyses.

Compared with conventional acid-based fractionation systems, the present method therefore provides several important advantages including higher biomass utilization efficiency, reduced cellulose degradation, preservation of crystalline cellulose integrity, lower chemical harshness, environmentally benign processing conditions and competitive nanocellulose production efficiency [23,24].

These findings collectively demonstrate that the DES-assisted extraction route developed in this study represents a highly effective and sustainable alternative for the production of high-quality nanocellulose from peanut shell

ARTICLE IN PRESS

agricultural waste. The combination of high extraction yield, high nanocellulose conversion efficiency, preserved crystallinity, favorable colloidal stability, and well-defined nanoscale morphology highlights the significant promise of this approach for future large-scale bio-based material production and advanced nanocellulose applications.

2.3. Characterization of Cellulose and CNPs

2.3.1. Experimental Runs and Measurement Repeatability

A total of 18 experimental runs were conducted in the present study, comprising eight experimental conditions for DES-assisted cellulose extraction (Table 1) and ten experimental conditions for subsequent nanocellulose production (Table 2). The experimental runs represent different processing conditions rather than independent replicate runs of every condition. Therefore, replicate processing was not performed for all experimental conditions. Repeatability was, however, incorporated into selected instrumental measurements. Zeta-potential measurements were performed in triplicate and the average values were reported, while DLS data were collected from three consecutive 60-s measurement runs. For morphological analysis, 50 individual fiber-diameter measurements were obtained per sample from FE-SEM images. The instrumental acquisition parameters and measurement resolutions used for FT-IR, FE-SEM, TEM, DLS, XRD, and zeta-potential analyses are specified in the corresponding characterization subsections below.

2.3.2. Chemical Structure FT-IR (Fourier-Transform Infrared Spectroscopy)

FT-IR spectra were recorded using a Thermo Nicolet AVATAR 370 spectrometer (Thermo Fisher Scientific, USA) in transmission mode. Samples were mixed with potassium bromide (KBr at a 1:100 (W/W) ratio and pressed into pellets using a hydraulic press at 10 tons for 5 min. Spectra were acquired over 4000–400 cm^{-1} at a spectral resolution of 4 cm^{-1} using 32 scans per sample. Baseline correction and peak identification were performed using OMNIC software.

2.4.2. Morphology (Field Emission Scanning Electron Microscopy, FE-SEM)

The morphology of the extracted cellulose and nanocellulose was examined using a Zeiss LEO 1450VP scanning electron microscope (Zeiss, Germany) operated at an accelerating voltage of 10–15 kV. Samples were mounted on aluminum stubs and sputter-coated with an approximately 10-nm gold layer using a Quorum SC7620 sputter coater. Images were acquired at magnifications ranging from 1,000× to 50,000×. Fiber diameters were quantified using ImageJ software based on 50 individual measurements per sample (n = 50).

2.3.5. Morphology Transmission electron microscopy (TEM)

Transmission electron microscopy was performed using a Philips CM120 transmission electron microscope at room temperature (20 °C), with images acquired over a magnification range of 31× to 680,000×.

2.3.6. Particle Size Distribution (Dynamic Light Scattering, DLS)

Hydrodynamic size distributions were measured using a Vasco3 nanoparticle size analyzer (Cordouan Technologies, France), equipped with a 658-nm laser diode operating at 65 mW. Measurements were performed at a scattering angle of 173° and a temperature of 25 °C. Samples were diluted to 0.1% (w/v) in deionized water and sonicated for 5 min prior to measurement to minimize the influence of loosely associated aggregates. For repeatability of the instrumental measurement, data were collected over three consecutive runs of 60 s each. The resulting intensity-weighted size distributions and polydispersity index (PDI) were processed using NanoQ software.

ARTICLE IN PRESS

2.3.7. Crystalline Structure (X-ray Diffraction, XRD)

XRD patterns were obtained using a GNR Explorer diffractometer (GNR Analytical Instruments, Italy) equipped with Cu Kα radiation (λ = 1.541874 Å), operated at 40 kV and 30 mA. Powdered samples were packed into a flat sample holder and scanned from 5° to 50° (2θ) with a step size of 0.05° and a scan rate of 2°/min. The crystallinity index (CrI) was calculated using the Segal equation (4).

$$CrI(\%) = \frac{I_{200} - I_{am}}{I_{200}} \times 100 \quad (4)$$

where I_{200} is the intensity of the (200) peak at ≈22.5° 2θ, and I_{am} is the amorphous intensity at ≈18° 2θ. Peak deconvolution was performed using OriginPro software if needed.

2.3.8. Zeta Potential Measurement

The zeta potential of the nanocellulose suspension was measured using a HORIBA SZ-100 (Horiba Scientific, Japan), based on the electrophoretic light scattering (ELS) technique. Measurements were performed at 25 °C using disposable zeta cells. Prior to analysis, the samples were diluted with deionized water to an appropriate concentration to minimize multiple scattering effects and ensure reliable results. An external electric field was applied to induce particle motion, and the electrophoretic mobility was determined from the Doppler shift of scattered light. The zeta potential values were then calculated using the Smoluchowski equation. Each measurement was conducted in triplicate to ensure reproducibility, and the average values were reported

3. Results and discussion

This study demonstrates the effective valorization of peanut shell waste into high-purity cellulose and cellulose nanoparticles using a choline chloride: urea DES pretreatment followed by probe-ultrasonication-assisted mechanical disintegration. The process was characterized through FTIR, FESEM, DLS, and XRD, revealing successful delignification, preserved cellulose integrity, and formation of nanoscale cellulose structures. These findings highlight the potential of DES as a green alternative for biomass processing.

3.1. Research Hypotheses

Based on the reported limitations of conventional chemical routes for nanocellulose production and the potential of deep eutectic solvents for lignocellulosic biomass fractionation, the present study was formulated around the following hypotheses: (i) choline chloride: urea deep eutectic solvent pretreatment can effectively remove non-cellulosic components from peanut shell biomass and provide a cellulose-rich fraction with a sufficiently preserved crystalline structure; (ii) subsequent probe ultrasonication can mechanically disintegrate the extracted cellulose into nanoscale cellulose particles without requiring acid or enzymatic hydrolysis; and (iii) the combination of DES-assisted fractionation and mechanical disintegration can produce cellulose nanoparticles with measurable nanoscale morphology, preserved cellulose I crystallinity, and favorable colloidal characteristics. These hypotheses were evaluated through cellulose yield determination and complementary FT-IR, FE-SEM, TEM, XRD, DLS, and zeta-potential analyses.

3.2. Optimization of Deep Eutectic Solvent-Assisted Cellulose Extraction and Ultrasonication-Mediated Cellulose Nanoparticle Production

ARTICLE IN PRESS

Table 3. Experimental design matrix and cellulose yield obtained from deep eutectic solvent-assisted extraction under different processing conditions.

Run Number	DES molar ratio (ChCl: Urea)	Temperature (°C)	Reaction time (h)	H_2O_2	Bleaching time (min)	Cellulose yield (%)
1	**2:1**	**90**	**3**	**3**	**30**	**50**
2	1:1	90	3	3	30	37
3	2:1	90	3	5	30	40
4	1:1	90	3	5	30	38
5	2:1	70	3	5	30	10
6	2:1	70	3	5	30	14
7	1:1	100	3	5	30	21
8	2:1	100	3	5	30	26

The effect of deep eutectic solvent composition and extraction parameters on cellulose recovery from peanut shell powder was investigated using a design of experiments approach. Different molar ratios of choline chloride to urea, extraction temperatures, hydrogen peroxide concentration, and bleaching conditions were evaluated, and the obtained cellulose yields are summarized in Table 4 The results demonstrated that the DES composition and extraction temperature had a significant influence on cellulose recovery. Among the evaluated conditions, the highest cellulose yield (50%) was achieved in Run 1 using a ChCl: Urea molar ratio of 2:1 at 90 °C for 3 h with 3% H_2O_2 and 30 min bleaching time. The superior performance of this DES composition can be attributed to the formation of an extensive hydrogen-bonding network between choline chloride and urea, which enhances the disruption of lignin–hemicellulose interactions and facilitates the liberation of cellulose fibers from the lignocellulosic matrix. Increasing the temperature beyond the optimum level did not further improve cellulose recovery, probably due to partial degradation of cellulose chains and the formation of soluble degradation products. These findings indicate that controlled DES pretreatment conditions are essential for achieving efficient cellulose isolation while preserving the polymeric structure.

ARTICLE IN PRESS

Table 4. Optimization of ultrasonication parameters for cellulose nanoparticle production from extracted cellulose and corresponding CNP yields.

Run number	Suspension time (h)	Sonication time (h)	Hydration Time (h)	CNP yield (%)
1	**1**	**3**	**12**	**80**
2	0.5	3	12	71
3	1	2	12	55
4	0.5	2	12	49
5	1	4	12	80
6	0.5	4	12	73
7	1	3	12	70
8	0.5	3	12	77

9	1	3	6	61
10	0.5	3	6	69

Following cellulose extraction, the purified cellulose was subjected to probe ultrasonication to obtain cellulose nanoparticles. The influence of suspension time, sonication duration, and hydration time on nanocellulose yield was evaluated, and the experimental results are presented in Table 5 The obtained results revealed that ultrasonication time was a critical parameter affecting the conversion of extracted cellulose into nanoscale structures. The highest nanocellulose yield (80%) was obtained in Runs 1 and 5, where the suspension and sonication times were optimized. The enhanced yield at prolonged sonication periods can be attributed to the cavitation phenomenon generated by ultrasonic waves, which promotes mechanical disintegration of the cellulose structure and reduces the dimensions of the resulting cellulose structures. However, excessive sonication did not result in a significant increase in yield, suggesting that a balance between energy input and structural preservation is required to prevent possible degradation of cellulose chains. The hydration period also affected nanocellulose formation, where insufficient hydration time resulted in lower yields due to incomplete swelling and dispersion of the extracted cellulose before ultrasonic treatment. Based on these findings, optimized ultrasonication conditions were selected for efficient conversion of extracted cellulose into nanocellulose.

3.3. Fourier-Transform Infrared (FT-IR) Spectroscopy Analysis

The Fourier-transform infrared (FT-IR) spectra of commercial cellulose (Cellulose1), DES-extracted and pretreated cellulose (Cellulose2), and the resulting nanocellulose (Nano Cellulose) are presented in Fig 4. A comparative evaluation of these spectra provides deeper insight into the progressive chemical purification and structural evolution of cellulose during DES pretreatment and subsequent nanoparticle formation.

All three spectra exhibit the characteristic vibrational features of cellulose, confirming that the fundamental polysaccharide backbone is preserved throughout the entire processing sequence. The broad absorption band centered at approximately 3330 cm^{-1}, attributed to O–H stretching vibrations, reflects the extensive intra- and intermolecular hydrogen bonding network inherent to cellulose [25]. Notably, this band becomes broader and slightly more intense in the nanocellulose sample, which can be ascribed to the increased exposure of hydroxyl groups resulting from fibrillation and particle size reduction. This enhancement in hydroxyl accessibility promotes stronger hydrogen bonding interactions, a phenomenon commonly reported for nanoscale cellulose materials with high specific surface area [26].

The absorption bands at 2920 cm^{-1} and 2850 cm^{-1} correspond to asymmetric and symmetric C–H stretching vibrations of aliphatic CH_2 groups within the glucopyranose units [27]. The persistence and minimal variation of these peaks across all samples indicate that the core glucopyranose ring structure remains chemically intact during DES treatment and mechanical disintegration. This observation highlights the non-destructive nature of the DES system toward the cellulose backbone, in contrast to harsher chemical treatments that may induce chain scission or depolymerization[22,28] .

A critical distinction between Cellulose1 and Cellulose2 is observed in the region around 1730 cm^{-1}, which is associated with C=O stretching vibrations of acetyl and ester groups present in hemicellulose [29]. The noticeable reduction of this peak in Cellulose2 confirms the effective removal of hemicellulosic components during DES pretreatment. In parallel, the absence of characteristic lignin-associated peaks at approximately 1505 cm^{-1} and 1600 cm^{-1} attributed to aromatic skeletal vibrations [30]in both Cellulose2 and Nano Cellulose provides strong evidence

ARTICLE IN PRESS

of successful delignification. These spectral changes collectively demonstrate the high selectivity of the DES system in removing amorphous matrix components while preserving the cellulose framework, consistent with the reported hydrogen-bond disruption mechanism of DES-based fractionation [18,19].

The band located in the range of 1640–1660 cm^{-1}, assigned to the bending vibration of adsorbed water (H–O–H), becomes more pronounced in the nanocellulose sample. This behavior reflects the increased surface area and hydrophilicity of nanocellulose, which enhances its ability to adsorb moisture from the surrounding atmosphere [31]. Such behavior is a typical characteristic of nanocellulose materials and is directly linked to their high density of accessible hydroxyl groups.

In the fingerprint region (1200–1000 cm^{-1}), all samples display strong and well-defined peaks corresponding to C–O–C glycosidic bond stretching (1050–1100 cm^{-1}) and C–O stretching vibrations within the pyranose ring [27,32]. However, these peaks become sharper and more intense in Cellulose2 and Nano Cellulose, indicating an increase in structural order and chemical purity following the removal of amorphous lignin and hemicellulose. This sharpening effect is often interpreted as a signature of improved molecular organization and reduced structural heterogeneity in purified cellulose systems [26].

Furthermore, the peak at approximately 1420 cm^{-1}, assigned to CH_2 bending vibrations and commonly used as an indicator of crystalline cellulose I structure, becomes relatively more prominent in the treated cellulose and nanocellulose samples [26]. This suggests an increase in relative crystallinity, which can be attributed to the preferential removal of amorphous components during DES pretreatment. Importantly, no significant shifts in peak positions are observed across the spectra, confirming that no new functional groups are introduced and that the chemical identity of cellulose remains unchanged during subsequent nanoparticle formation.

Overall, the FT-IR results provide compelling evidence that DES pretreatment enables efficient and selective removal of non-cellulosic components, while preserving the intrinsic chemical structure of cellulose. The subsequent nanoparticle formation process primarily induces physical and morphological changes such as increased surface area and enhanced hydrogen bonding without altering the fundamental molecular framework. These findings further support the suitability of DES-based strategies as a green and structurally preserving approach for producing high-quality nanocellulose from lignocellulosic biomass [18,19].

The FT-IR results obtained in this study are in good agreement with previous reports on peanut shell-derived cellulose and nanocellulose systems prepared via conventional chemical treatments. For instance, Terea et al. reported the gradual disappearance of hemicellulose- and lignin-related bands near 1730 cm^{-1} and 1500–1600 cm^{-1} following acid–alkali purification and sulfuric acid hydrolysis of peanut shell biomass, confirming efficient removal of amorphous components. However, unlike those harsh chemical approaches involving concentrated H_2SO_4, HCl, and NaOH treatments, the present DES-assisted system achieved comparable purification while preserving the native cellulose backbone without noticeable structural degradation. Similar preservation of cellulose characteristic bands has also been reported for nanocellulose prepared from agricultural residues using TEMPO-mediated oxidation and alkaline extraction routes [33]. Nevertheless, the current DES-based approach offers a greener and less corrosive alternative, while still maintaining high chemical selectivity toward lignin and hemicellulose removal. The enhanced intensity and sharpening of cellulose-associated peaks observed here further suggest improved structural organization and hydrogen-bond integrity compared with several previously reported acid-hydrolyzed systems.

ARTICLE IN PRESS

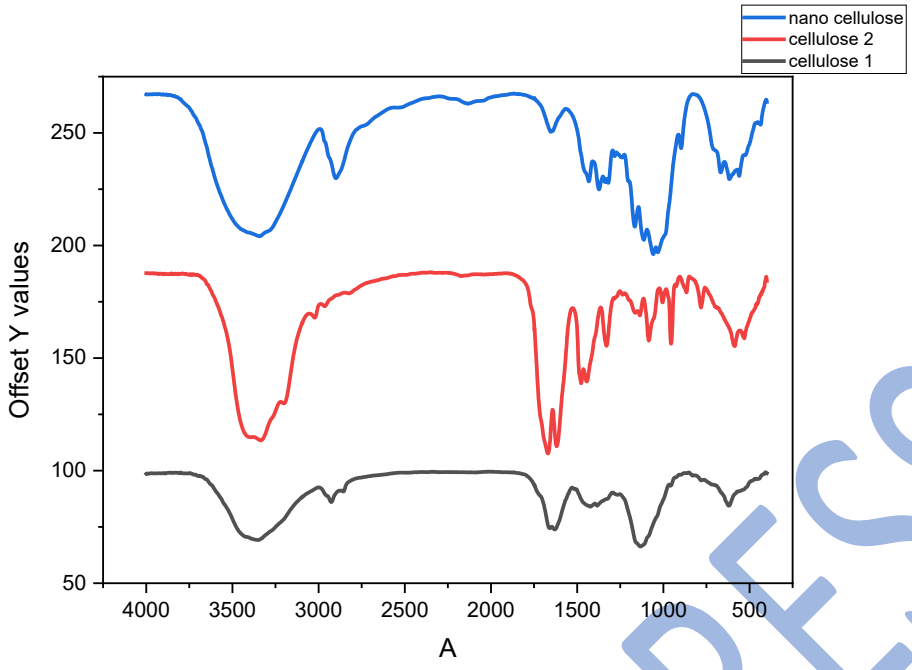


Fig 4. FT-IR spectra of (Cellulose1) commercial cellulose (black), (Cellulose2) DES-extracted and pretreated cellulose (red), and nanocellulose (blue)

3.4. Morphological Analysis of Extracted Cellulose and Derived Nanocellulose (FE-SEM)

Field-Emission Scanning Electron Microscopy (FE-SEM) was employed to visualize the stepwise morphological transformation of peanut shell waste throughout the integrated deep eutectic solvent (DES) pretreatment and ultrasonication-assisted mechanical disintegration process. The micrographs in Fig 5. provide direct evidence of structural deconstruction at various stages.

The low-magnification image (Fig 5a) reveals that the DES pretreatment fundamentally altered the biomass architecture, resulting in a highly porous and interconnected fibrillar network. This macro-porosity is a direct physical consequence of the efficient removal of lignin and hemicellulose which otherwise act as a binding matrix and serves as a hallmark of successful delignification using selective solvents like DES [33,34]. At higher magnification (Fig 5b), individual cellulose microfibrils appear with smooth, clean surfaces and clear separation. The absence of amorphous debris or surface coatings confirms the high purity of the extracted cellulose, corroborating the FT-IR findings. This suggests that the DES selectively dissolved non-cellulosic components without causing significant erosion to the crystalline cellulose surfaces. These microfibers, with an average diameter in the micrometer range (5–20 µm), serve as the essential precursor for nanocellulose production [27,31].

Following probe ultrasonication, a clear transition toward the nanoscale is observed. Fig 5c illustrates the formation of an intricate web-like network of nanocellulose, signifying the successful breakdown of the larger fiber bundles. At the highest magnification (Fig 5d), the material is resolved into individual cellulose nanoparticles (CNPs) exhibiting a needle-like morphology. Statistical analysis indicates an average diameter in the range of 10–40 nm, representing a reduction of two to three orders of magnitude compared with the extracted cellulose prior to ultrasonication. The formation of these nanoscale structures is attributed primarily to the mechanical effects of ultrasonic cavitation, which disrupts intermolecular and interfibrillar interactions and promotes the disintegration of the cellulose structure into nanoscale cellulose particles [16].

The morphology of the DES-extracted cellulose and the resulting CNPs aligns with, and often appears more defined than, structures reported in studies using conventional strong alkalis, which frequently cause excessive swelling and

ARTICLE IN PRESS

surface pitting [7]. Specifically, the observed nanoscale particle morphology demonstrates the green yet effective nature of DES in preserving fibrillar integrity while achieving efficient formation of nanoscale cellulose particles [35]. This preserved structural integrity and nanoscale morphology indicate that peanut shell-derived CNPs may have potential as functional components in advanced cellulose-based composites.

The morphological features observed in the present study are highly consistent with previously reported peanut shell-derived nanocellulose systems, where fibrillar and partially individualized nanostructures were obtained following acid hydrolysis and alkaline delignification treatments [36]. However, many conventional extraction routes often produce fibers with severe surface erosion, aggregation, or irregular fragmentation due to the aggressive nature of strong mineral acids and oxidizing agents [7,16]. In contrast, the DES-mediated pretreatment employed in this work resulted in cleaner fibrillar surfaces, reduced structural collapse, and more homogeneous nanoparticle formation, indicating that the cellulose crystalline domains were preserved more effectively during biomass fractionation. The observed nanofibrillar morphology and high aspect ratio are also comparable to those reported for nanocellulose extracted from other lignocellulosic agricultural wastes such as rice husk, sugarcane bagasse, and corn stover [16]. These findings collectively demonstrate that the DES-based strategy provides an environmentally benign yet structurally efficient route for producing high-quality nanocellulose from peanut shell biomass.

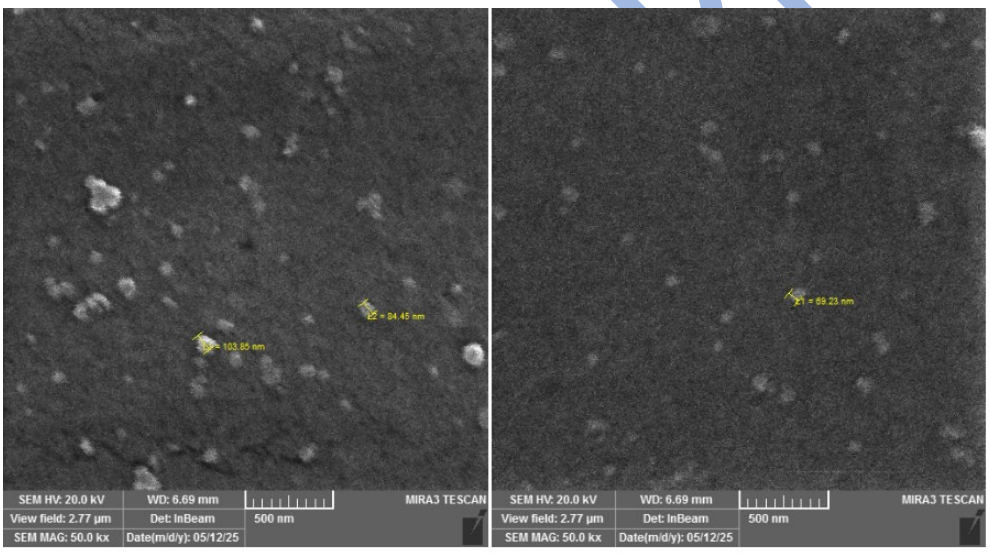


Fig 5. FE-SEM micrographs of peanut shell-derived cellulose at different processing stages: (a) Low-magnification view showing the macroporous fibrillar network of cellulose after DES pretreatment. (b) High-magnification image of individual cellulose microfibrils with separated fibrillar structure. (c) Nanoscale cellulose network after probe ultrasonication and mechanical disintegration. (d) High-resolution image of cellulose nanoparticles (CNPs) showing their nanoscale dimensions and particle-like morphology.

3.5. Transmission electron microscopy (TEM)

Transmission electron microscopy (TEM) was employed to investigate the morphology of the nanostructures obtained after DES treatment of peanut shell biomass. The TEM micrographs reveal the presence of nanoscale cellulose structures with heterogeneous morphology distributed throughout the matrix. Distinct nanostructured domains with approximately rounded to ellipsoidal shapes are observed alongside partially fibrillated regions, indicating that the DES pretreatment effectively disrupted the compact lignocellulosic structure and promoted the liberation of cellulose nanostructures. According to the scale bars (90–100 nm), the dimensions of these nanostructured domains fall within the nanometric range, confirming the successful formation of nanoscale cellulose particles. In several areas, thin fibrillar connections between adjacent domains can also be distinguished, suggesting partial defibrillation of cellulose

bundles during the treatment process. Moreover, localized agglomerated regions are visible in the micrographs, which can be attributed to the strong intermolecular hydrogen bonding and high surface energy of cellulose nanostructures, leading to partial aggregation during drying or TEM sample preparation. Overall, the TEM observations demonstrate that the DES-assisted treatment facilitates the breakdown of the lignocellulosic matrix and the generation of nanoscale cellulose structures, supporting the effectiveness of this environmentally benign extraction approach [16].

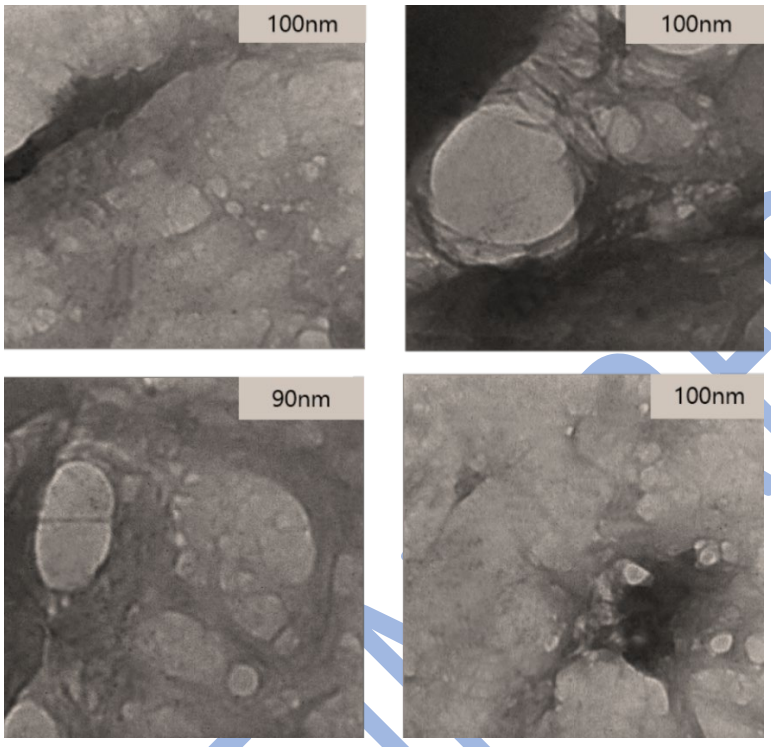


Fig 6. TEM images of nanocellulose extracted from peanut shell via deep eutectic solvent (DES) treatment, showing nanoscale cellulose particles and partially interconnected structures. Scale bars: 100 nm and 90 nm.

3.6. Dynamic Light Scattering (DLS) Analysis

Dynamic light scattering (DLS) was employed to quantitatively assess the hydrodynamic size distribution and to further confirm the conversion of micro-scale cellulose into nanoscale cellulose particles in aqueous suspension. The intensity-weighted size distributions for both suspensions are shown in Fig 7.

For the DES-extracted cellulose suspension (Fig. 7a), the DLS profile exhibits a broad, polydisperse distribution spanning the micrometer range. A predominant, wide peak is centered between approximately 2,000 and 5,000 nm, with a pronounced tail extending beyond 10,000 nm. The large hydrodynamic diameters, together with a high polydispersity index (PDI > 0.45), are characteristic of partially aggregates of microscale cellulose structures rather than nanoscale cellulose particles dispersed in water [35]. These observations are consistent with the nanoparticle cellulose network observed in the FE-SEM micrographs (Fig. 5a, b), confirming that the dispersed entities at this stage are mainly aggregates of cellulose microparticle rather than individualized nanoparticle.

In contrast, the DLS analysis of the nanocellulose suspension (Fig. 7b) reveals a clear shift toward smaller sizes. The intensity distribution is dominated by a peak in the 120–180 nm range, indicating that the majority of scattered intensity arises from nanoscale entities. The Z-average hydrodynamic diameter is 833.15 nm with a PDI of ~0.5, suggesting that, although a fraction of the nanoparticles exists as relatively small aggregates, the overall size distribution remains moderately polydisperse. The presence of a small comb in the micrometer range most likely refers to a small population of residual aggregates or incomplete fibril fragments that have not yet been converted

into cellulose nanoparticles, which is commonly observed in nanocellulose suspensions prepared by mechanical and/or chemical disintegration. [36,37].

It should be noted that DLS measures the hydrodynamic diameter of scattering objects in suspension and is strongly biased toward larger particles or aggregates, whereas FE-SEM provides direct visualization of the dry morphology and the particle diameters. Therefore, the higher Z-average value and PDI obtained by DLS do not contradict the nanoscale diameters observed by FE-SEM; instead, they reflect the presence of loosely associated nanoparticle bundles and dynamic aggregation in the aqueous phase. Taken together, the FE-SEM and DLS results provide complementary evidence that the DES treated cellulose undergoes a transition from a polydisperse, microparticle network to a nanostructured suspension dominated by nanoparticles, with only limited residual aggregation.

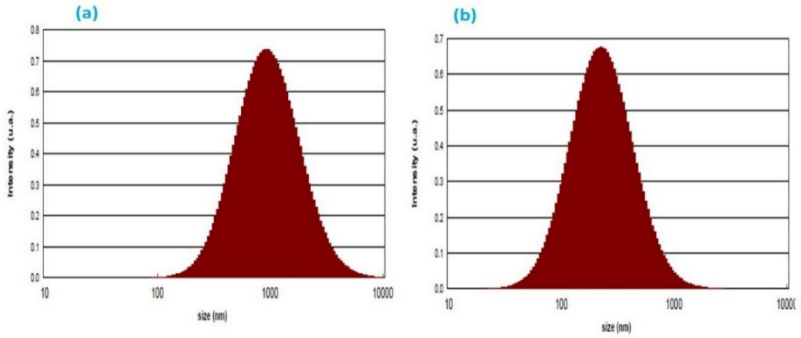


Fig 7. Intensity-weighted hydrodynamic size distributions from DLS analysis: (a) DES-extracted cellulose suspension (b) Nanocellulose suspension

3.7. X-ray Diffraction (XRD) Analysis

The X-ray diffraction patterns of the purified cellulose and the obtained nanocellulose derived from peanut shell biomass are presented in Fig 8 and 9. Both samples exhibited the characteristic diffraction peaks of native cellulose I, demonstrating that the crystalline polymorph of cellulose was successfully preserved throughout the DES-assisted extraction and subsequent nanoparticle formation process [37]. The purified cellulose displayed relatively broad diffraction peaks centered at approximately $2\theta = 16°$ and 22°, corresponding to the overlapping (110)/($1\bar{1}0$) and the (002) crystallographic planes of cellulose I, respectively. A weak diffraction feature was also observed in the 34–35° region, which is commonly assigned to the (004) plane. The broad nature of these reflections indicates the coexistence of crystalline and amorphous domains within the extracted cellulose, suggesting that although lignin and hemicellulose were efficiently removed during pretreatment, a considerable fraction of disordered cellulose regions remained. In contrast, the nanocellulose sample exhibited noticeably sharper and more intense diffraction peaks while maintaining the characteristic cellulose I crystal structure. The dominant reflection appeared at $2\theta = 22.65°$, corresponding to the (002) plane, whereas the diffraction peaks near 16° and 34–35° remained clearly distinguishable. The increased intensity and reduced peak broadening indicate a higher degree of structural ordering and improved crystalline organization after nanoparticle formation. The enhancement in crystallinity can be attributed to the selective removal of non-cellulosic components and loosely organized amorphous cellulose regions during the DES-assisted pretreatment, together with the effective mechanical disintegration process that increased the relative exposure of highly ordered cellulose domains. As a result, the relative proportion of crystalline domains increased, producing a more organized cellulose network while preserving the native cellulose polymorph[34]. The crystallinity index (CrI), calculated using the Segal method, reached approximately 81.1%, confirming the successful production of highly crystalline nanocellulose. This value is comparable to or higher than those reported for nanocellulose isolated from various lignocellulosic agricultural residues, demonstrating the effectiveness of the employed green

ARTICLE IN PRESS

processing strategy [16]. The preservation of the cellulose I crystalline structure together with the substantial increase in peak intensity, peak sharpness, and crystallinity provides strong evidence for the successful conversion of purified cellulose into nanocellulose. Although XRD analysis alone cannot directly determine particle dimensions, the observed structural evolution is fully consistent with the nanoscale morphology identified by FE-SEM and TEM analyses and with the particle size distribution obtained from DLS measurements. Overall, the XRD results demonstrate that the choline chloride: urea deep eutectic solvent efficiently fractionated the peanut shell biomass while preserving the intrinsic crystalline structure of cellulose. The subsequent nanoparticle formation process further enhanced the crystalline organization, resulting in highly ordered nanocellulose with minimal structural degradation and excellent physicochemical characteristics suitable for advanced material applications.

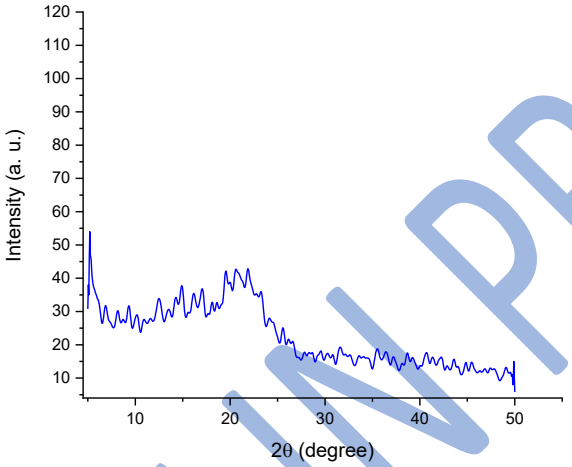


Fig 8. X-ray diffraction pattern of cellulose extracted from peanut shells using a deep eutectic solvent (DES). Characteristic diffraction peaks of cellulose I were detected at approximately 2θ = 16°, 22°, and 34–35°, corresponding to the (110), (002), and (004) crystal planes, respectively. The broad nature of the diffraction peaks reflects the presence of both crystalline and amorphous cellulose domains, confirming the successful isolation of cellulose while maintaining its native crystalline structure.

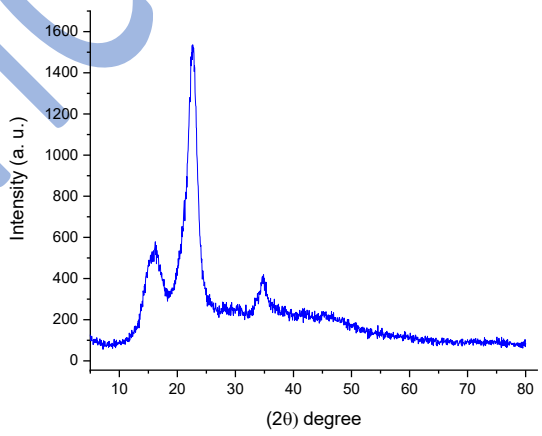


Fig 9. X-ray diffraction pattern of cellulose nanoparticles obtained from cellulose extracted from peanut shells using a deep eutectic solvent (DES). Characteristic diffraction peaks of cellulose I were detected at approximately 2θ = 16°, 22.65°, and 34–35°, corresponding to the (110), (002), and (004) crystal planes, respectively. The enhanced intensity and sharpness of the (002) reflection indicate increased crystallinity and successful nanocellulose formation.

ARTICLE IN PRESS

3.8. Zeta potential analysis

The zeta potential of the nanocellulose suspension was measured to evaluate its colloidal stability and surface charge characteristics. The obtained results (Fig 10.) show negative zeta potential values ranging from approximately −27 to −35 mV, with an average value close to −30 mV. Such negative surface charge is characteristic of cellulose-based nanomaterials and arises from the presence of hydroxyl groups and possible formation of weakly ionized surface functionalities during processing [38].

The magnitude of the zeta potential indicates that the nanocellulose suspension exhibits moderate to good colloidal stability. In particular, the sample with a zeta potential of −34.9 mV approaches the threshold commonly associated with highly stable dispersions, where strong electrostatic repulsion prevents particle aggregation [27]. This behavior suggests that the produced nanocellulose can form relatively stable aqueous suspensions, which is a desirable feature for applications in nanocomposites, coatings, and biomedical systems.

The slight variation observed between repeated measurements (−27 to −35 mV) may be attributed to differences in dispersion homogeneity and the presence of minor aggregates, as also indicated by the occasional appearance of secondary peaks in the distribution profile. Such behavior is typical for nanocellulose systems, where strong hydrogen bonding interactions can lead to partial fibril association in aqueous media.

Overall, the negative zeta potential values confirm that the DES-assisted process not only preserves the chemical structure of cellulose but also yields nanocellulose with sufficient surface charge to ensure dispersion stability. This electrostatic stabilization, combined with the high surface area of nanoparticles, enhances their suitability for advanced applications requiring stable colloidal systems.

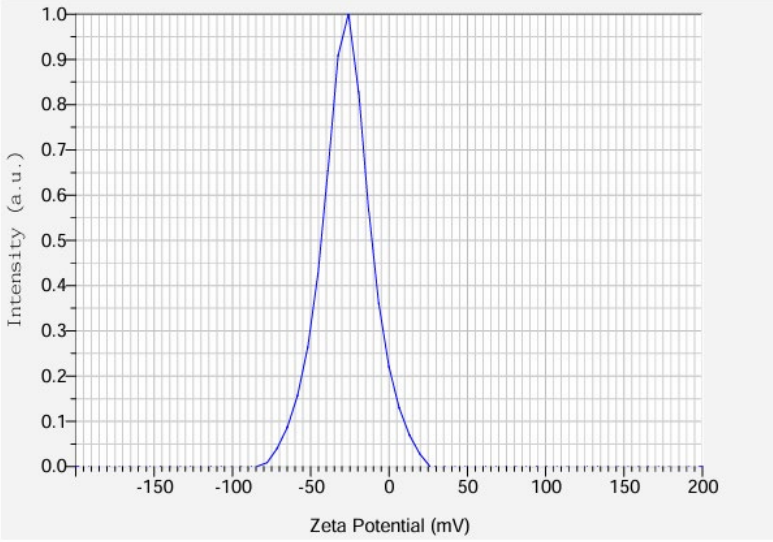


Fig 10. Zeta potential distribution of nanocellulose suspension, demonstrating a negative surface charge and good colloidal stability in aqueous medium.

3.9. Comparison with Previously Reported Nanocellulose Production Routes

Although deep eutectic solvent (DES)-based pretreatment has increasingly been investigated for the fractionation of lignocellulosic biomass, previously reported approaches have employed different combinations of chemical pretreatment, acid hydrolysis, oxidation, and mechanical fibrillation. For example, DES-based processing of peanut shells has previously been reported for the preparation of lignin-containing cellulose nanocrystals [13], while other studies have combined alkaline pretreatment with acid hydrolysis and ultrasonication [14] or employed acid

ARTICLE IN PRESS

hydrolysis as the principal nanocellulose isolation step [24]. More recently, ChCl-based DES systems combined with intensive ultrasonication have been investigated for the production of cellulose nanofibers from barley straw [10,39]. The present study differs from these approaches primarily in the configuration of the nanoparticle formation stage. In the proposed route, choline chloride: urea DES was first employed for fractionation and purification of peanut shell biomass, followed by probe-ultrasonication-assisted mechanical disintegration without the use of acid or enzymatic hydrolysis. Thus, nanoscale cellulose particle formation in the present process is achieved predominantly through the mechanical effects associated with ultrasonic cavitation rather than through chemical cleavage of cellulose chains. This distinction provides a simpler nanoparticle formation pathway and avoids the use of strong mineral acids during the conversion of purified cellulose into nanocellulose.

As summarized in Table 6, the present approach produced approximately 50% cellulose from the initial peanut shell biomass, followed by an approximately 80% conversion of the extracted cellulose to nanocellulose, corresponding to an overall yield of approximately 40%. The resulting nanocellulose exhibited fibrillar dimensions of approximately 10–40 nm and a crystallinity index of 81.1%, while the negative zeta potential values of −27 to −35 mV indicated moderate to good colloidal stability. These characteristics compare favorably with several previously reported lignocellulosic nanocellulose systems, although direct comparison of yield values should be made with caution because the reported yields in the literature are not always calculated on the same basis. Importantly, the preservation of the cellulose I crystalline structure together with nanoscale fibrillation demonstrates that effective nanocellulose production can be achieved without introducing an acid-hydrolysis step into the nanoparticle formation stage.

Overall, the results indicate that the proposed ChCl: urea DES-assisted extraction followed by probe-ultrasonication-assisted mechanical defibrillation provides a distinct and potentially simplified route for converting peanut shell waste into nanocellulose. The combination of relatively high cellulose recovery, substantial conversion of the extracted cellulose to nanocellulose, preservation of cellulose I crystallinity, nanoscale fibrillar morphology, and favorable colloidal characteristics highlights the potential of this integrated approach for the valorization of peanut shell biomass.

ARTICLE IN PRESS

Table 5. Comparison of the present approach with selected previously reported routes for nanocellulose production from lignocellulosic biomass.

Entry	Study	Feedstock	Main pretreatment	nanoparticle formation	Yield (%)	Main feature and limitation
1	[23]	Groundnut shell	Chemical pretreatment	Chemical isolation of cellulose nanocrystals	12 % overall yield	Directly related to groundnut shell; relatively low overall CNC yield
2	[24]	Almond shell	Acid treatment	Acid hydrolysis	67–71.8% overall yield	High reported yield, but requires strong acid hydrolysis
3	[16]	Sugarcane bagasse	Alkaline treatment + H_2O_2 + mild H_2SO_4 hydrolysis	Ultrasonication-assisted fibrillation	42% overall yield	Effective nano fibrillation but involves multiple chemical treatment steps, including acid hydrolysis
4	[13]	Peanut shell	ChCl-based DES containing lignin-derived phenol	Preparation of lignin-containing cellulose nanocrystals	59.49% overall yield	Peanut-shell-based DES route; performed at 120 °C for 3 h and produced lignin-containing CNCs
5	[10]	Barley straw	ChCl: formic acid DES	Wet grinding + high-intensity ultrasonication	>80% nano fibrillation	DES-assisted ultrasound route; requires intensive mechanical processing
6	[39]	Barley straw	ChCl–oxalic acid dihydrate DES	Wet grinding + high-intensity ultrasonication	>80% nano fibrillation	Cellulose purity >88%, PDI <0.5, and zeta potential <−30 mV
7	Present study	Peanut shell	ChCl: urea DES	Probe-ultrasonication-assisted mechanical disintegration	80% CNP conversion	Acid-free mechanical nanoparticle formation; preservation of cellulose I; comprehensive morphological, structural, and colloidal characterization

3.10. Potential Practical Applications

The characteristics of the nanocellulose obtained in this study suggest several potential real-world applications. The nanoscale morphology (10–40 nm), preserved cellulose I crystalline structure, and negative zeta potential indicate

that the produced nanocellulose could serve as a reinforcing and functional component in bio-based polymer matrices. In particular, its incorporation into biodegradable polymer films and nanocomposite materials could potentially improve mechanical reinforcement and contribute to the development of cellulose-based packaging materials. The nanoscale morphology and high crystallinity also make the material potentially suitable for use as a reinforcing phase in coatings and other cellulose-based composite systems. However, these potential applications were not directly evaluated in the present study. Therefore, application-specific studies should be conducted to determine the effects of nanocellulose loading, dispersion, interfacial compatibility, and processing conditions on the mechanical, barrier, and functional properties of the resulting materials.

4. Conclusion

In this study, peanut shell biomass was successfully converted into cellulose nanoparticles (CNPs) through an integrated choline chloride: urea deep eutectic solvent (DES) pretreatment followed by probe-ultrasonication-assisted mechanical disintegration. The DES pretreatment resulted in approximately 50% cellulose recovery from the initial peanut shell biomass, while subsequent probe ultrasonication converted approximately 80% of the extracted cellulose into CNPs, corresponding to an overall yield of approximately 40%. Importantly, nanoparticle formation was achieved without acid or enzymatic hydrolysis, with ultrasonic cavitation and mechanical disintegration serving as the principal mechanisms responsible for the formation of nanoscale cellulose particles. The structural and morphological analyses confirmed the successful formation of nanostructured cellulose. FE-SEM revealed nanoscale cellulose structures with characteristic dimensions of approximately 10–40 nm, while TEM further confirmed nanoscale cellulose structures with particle-like morphology. XRD analysis showed that the cellulose I crystalline structure was retained, with a crystallinity index of approximately 81.1%. DLS analysis indicated a dominant hydrodynamic size distribution in the 120–180 nm range, whereas the Z-average diameter of 833.15 nm and PDI of approximately 0.5 suggested the presence of associated nanoparticles and aggregates in the aqueous suspension. In addition, the CNPs exhibited negative zeta-potential values ranging from −27 to −35 mV, indicating moderate to good colloidal stability.

The proposed process provides a distinct processing configuration in which DES-assisted fractionation is followed by chemical-hydrolysis-free mechanical disintegration. Compared with conventional routes involving acid hydrolysis, alkaline treatment, or oxidative processing, this approach avoids the use of chemical hydrolytic agents during the nanoparticle formation step while maintaining the characteristic cellulose I structure and producing nanoscale cellulose particles. Despite these promising results, several limitations should be considered. First, the present study was conducted at laboratory scale, and therefore the scalability of the DES-assisted extraction and probe-ultrasonication process has not yet been established. Second, the energy consumption associated with prolonged probe ultrasonication was not systematically quantified, although sonication is an important operational step in the proposed route. Third, the DES recovery and recycling potential were not evaluated, and the environmental performance of the complete process was not assessed through a life-cycle analysis. In addition, although the produced CNPs showed favorable morphological and colloidal characteristics, their performance in specific end-use applications was not investigated in the present study. Future studies should therefore focus on process scale-up, optimization of sonication energy and time, DES recovery and recycling, and techno-economic and life-cycle assessments. Further investigation of the incorporation of the produced CNPs into polymeric matrices and the

ARTICLE IN PRESS

evaluation of their functional performance in application-specific systems would also be valuable for determining their practical potential. The resulting CNPs therefore represent a promising bio-based material for future development of polymer nanocomposites, biodegradable films, packaging materials, and cellulose-based coatings, although application-specific performance remains to be experimentally established.

Funding

The authors gratefully acknowledge the financial support provided by Islamic Azad University, Quchan Branch, Quchan, Iran.

Conflict of Interest

The authors declare that they have no conflict of interest.

Nomenclature

Abbreviation	Full form
CNPs	Cellulose Nanoparticles
CrI	Crystallinity Index
DES	Deep Eutectic Solvent
DLS	Dynamic Light Scattering
ELS	Electrophoretic Light Scattering
FE-SEM	Field Emission Scanning Electron Microscopy
FT-IR	Transform Infrared Spectroscopy Fourier
H_2O_2	Hydrogen Peroxide
PDI	Polydispersity Index
TEM	Transmission Electron Microscopy
XRD	X-ray Diffraction
ChCl	Choline Chloride
KBr	Potassium bromide
W/V	Weight/volume
V/V	Volume/Volume
Cu Kα	Copper K-alpha radiation

References

[1] Bhardwaj, M.K., Kumar, H., Khan, N.A., Goyal, S.K., 2026. Microplastics as emerging pollutants: ecological insights from aquatic systems and impacts on human health – A review, *International Journal of Environmental Quality*, 73, 130–141. https://doi.org/10.60923/issn.2281-4485/23554

[2] Soleimanzadeh, H., Salari, D., Olad, A., Ostadrahimi, A., 2025. Optimization of delignification and cellulose isolation process from natural cotton pods and preparation of its nanofibers with choline chloride–lactic acid eutectic solvents, *Biomass Conversion and Biorefinery*, 15, 2063–2079. https://doi.org/10.1007/s13399-023-04141-9

[3] Zhao, D., Zhu, Y., Cheng, W., Chen, W., Wu, Y., Yu, H., 2021. Cellulose-based flexible functional materials for emerging intelligent electronics, *Advanced Materials*, 33, 2000619. https://doi.org/10.1002/adma.202000619

[4] Zhu, J., Shao, C., Hao, S., Zhang, J., Ren, W., Wang, B., Xiao, L., Wang, C., Shao, L., 2025. Recent progress on the dissolution of cellulose in deep eutectic solvents, *Industrial Crops and Products*, 228, 120844. https://doi.org/10.1016/j.indcrop.2025.120844

[5] Joseph, B., S.V.K., S., Sabu, C., Kalarikkal, N., Thomas, S., 2020. Cellulose nanocomposites: Fabrication and biomedical applications, *Journal of Bioresources and Bioproducts*, 5, 223–237. https://doi.org/10.1016/j.jobab.2020.10.001

[6] Ling, S., Chen, W., Fan, Y., Zheng, K., Jin, K., Yu, H., Buehler, M.J., Kaplan, D.L., 2018. Biopolymer nanofibrils: Structure, modeling, preparation, and applications, *Progress in Polymer Science*, 85, 1–56. https://doi.org/10.1016/j.progpolymsci.2018.06.004

[7] Trache, D., Tarchoun, A.F., Derradji, M., Hamidon, T.S., Masruchin, N., Brosse, N., Hussin, M.H., 2020. Nanocellulose: From fundamentals to advanced applications, *Frontiers in Chemistry*, 8, 392. https://doi.org/10.3389/fchem.2020.00392

[8] Özbaş, K.E., 2026. Synergistic effects and pseudo-component behavior in ternary co-pyrolysis of low-rank coal with pectin- and lignin-rich agricultural residues, *Sustainability*, 18, 5465. https://doi.org/10.3390/su18115465

ARTICLE IN PRESS

[9] Khandaker, T., Islam, T., Nandi, A., Anik, M.A.A.M., Hossain, M.S., Hasan, M.K., Hossain, M.S., 2025. Biomass-derived carbon materials for sustainable energy applications: A comprehensive review, *Sustainable Energy & Fuels*, 9, 693–723. https://doi.org/10.1039/D4SE01393J
[10] Pradhan, D., Jaiswal, S., Tiwari, B.K., Jaiswal, A.K., 2024. Nanocellulose separation from barley straw via ultrasound-assisted choline chloride–formic acid deep eutectic solvent pretreatment and high-intensity ultrasonication, *Ultrasonics Sonochemistry*, 110, 107048. https://doi.org/10.1016/j.ultsonch.2024.107048
[11] Zhang, M., Wang, D., Wang, S., Du, H., Li, G., Lan, R., Li, Y., 2025. Resource utilization of peanut shells: Nutritional characteristics, regulation of antinutritional factors, and application potential in livestock and poultry production, *Food Science & Nutrition*, 13. https://doi.org/10.1002/fsn3.70994
[12] Ganguly, P., Sengupta, S., Das, P., Bhowal, A., 2020. Synthesis of cellulose from peanut shell waste and its use in bioethanol production, in: *Bioresource Utilization and Bioprocessing*, Springer, Singapore, pp. 81–91. https://doi.org/10.1007/978-981-15-1607-8_10
[13] Lu, A., Yu, X., Ji, Q., Chen, L., Yagoub, A.E.-G., Olugbenga, F., Zhou, C., 2023. Preparation and characterization of lignin-containing cellulose nanocrystals from peanut shells using a deep eutectic solvent containing lignin-derived phenol, *Industrial Crops and Products*, 195, 116415. https://doi.org/10.1016/j.indcrop.2023.116415
[14] Rajinipriya, M., Nagalakshmaiah, M., Robert, M., Elkoun, S., 2018. Importance of agricultural and industrial waste in the field of nanocellulose and recent industrial developments of wood based nanocellulose: A review, *ACS Sustainable Chemistry & Engineering*, 6, 2807–2828. https://doi.org/10.1021/acssuschemeng.7b03437
[15] Klemm, D., Kramer, F., Moritz, S., Lindström, T., Ankerfors, M., Gray, D., Dorris, A., 2011. Nanocelluloses: A new family of nature-based materials, *Angewandte Chemie International Edition*, 50, 5438–5466. https://doi.org/10.1002/anie.201001273
[16] Asem, M., Jimat, D.N., Jafri, N.H.S., Wan Nawawi, W.M.F., Mohamed Azmin, N.F., Abd Wahab, M.F., 2023. Entangled cellulose nanofibers produced from sugarcane bagasse via alkaline treatment, mild acid hydrolysis assisted with ultrasonication, *Journal of King Saud University – Engineering Sciences*, 35, 24–31. https://doi.org/10.1016/j.jksues.2021.03.003
[17] Syed Putra, S.S., Alias, Y., Basirun, W.J., Zainal Abidin, M.I.I., Hayyan, A., Siburian, R., 2026. Tunable deep eutectic solvents for biomass fractionation: Physicochemical insights and toxicity, *ChemBioEng Reviews*, 13. https://doi.org/10.1002/cben.70064
[18] Hussain, M., Ashraf, H.T., Vasudev, V., Yasin, S., Jamil, M.I., Saleem, M., Aziz, T., Al Afroz, E., Feichao, Z., Huapeng, Z., Bin, Y., 2025. Deep eutectic solvents in biomass pretreatment for green approach: A comprehensive review, *Polymer Bulletin*, 82, 10513–10552. https://doi.org/10.1007/s00289-025-05955-5
[19] Satlewal, A., Agrawal, R., Bhagia, S., Sangoro, J., Ragauskas, A.J., 2018. Natural deep eutectic solvents for lignocellulosic biomass pretreatment: Recent developments, challenges and novel opportunities, *Biotechnology Advances*, 36, 2032–2050. https://doi.org/10.1016/j.biotechadv.2018.08.009
[20] Sihag, S.S., Pal, J., Yadav, M., 2022. Extraction and characterization of nanocellulose from wheat straw: Facile approach, *Journal of Water and Environmental Nanotechnology*, 7, 317–331. https://doi.org/10.22090/jwent.2022.03.007
[21] Ibrahim, A., Abdullah, M.F., Sam, S.T., 2018. Hydrolysis empty fruit bunch (EFB) using green solvent, *IOP Conference Series: Materials Science and Engineering*, 429, 012059. https://doi.org/10.1088/1757-899X/429/1/012059
[22] Wang, J., Wang, Q., Wu, Y., Bai, F., Wang, H., Si, S., Lu, Y., Li, X., Wang, S., 2020. Preparation of cellulose nanofibers from bagasse by phosphoric acid and hydrogen peroxide enables fibrillation via a swelling, hydrolysis, and oxidation cooperative mechanism, *Nanomaterials*, 10, 2227. https://doi.org/10.3390/nano10112227
[23] Bano, S., Negi, Y.S., 2017. Studies on cellulose nanocrystals isolated from groundnut shells, *Carbohydrate Polymers*, 157, 1041–1049. https://doi.org/10.1016/j.carbpol.2016.10.069
[24] Alhaji Mohammed, M., Basirun, W.J., Abd Rahman, N.M.M., Shalauddin, M., Salleh, N.M., 2022. The effect of acid hydrolysis parameters on the properties of nanocellulose extracted from almond shells, *Journal of Natural Fibers*, 19, 14102–14114. https://doi.org/10.1080/15440478.2022.2116518
[25] Liu, Y., Deak, N., Wang, Z., Yu, H., Hameleers, L., Jurak, E., Deuss, P.J., Barta, K., 2021. Tunable and functional deep eutectic solvents for lignocellulose valorization, *Nature Communications*, 12, 5424. https://doi.org/10.1038/s41467-021-25117-1
[26] Hospodarova, V., Singovszka, E., Stevulova, N., 2018. Characterization of cellulosic fibers by FTIR spectroscopy for their further implementation to building materials, *American Journal of Analytical Chemistry*, 9, 303–310. https://doi.org/10.4236/ajac.2018.96023
[27] Yao, Z., Chong, G., Guo, H., 2024. Deep eutectic solvent pretreatment and green separation of lignocellulose, *Applied Sciences*, 14, 7662. https://doi.org/10.3390/app14177662
[28] Mehdigholami, S., Koohestanian, E., 2023. Fe3O4@SiO2/AEPTMS/Fe(OTf)3: An efficient superparamagnetic nanocatalyst for the protecting of alcohols, *Journal of Particle Science and Technology*, 9, 1–9. https://doi.org/10.22104/jpst.2023.6188.1224
[29] Baraka, F., Erdocia, X., Velazco-Cabral, I., Hernández-Ramos, F., Dávila-Rodríguez, I., Maugin, M., Labidi, J., 2024. Impact of deep eutectic solvent pre-treatment on the extraction of cellulose nanofibers, *Cellulose*, 31, 9645–9660. https://doi.org/10.1007/s10570-024-06185-0
[30] Sirviö, J.A., Hyypiö, K., Asaadi, S., Junka, K., Liimatainen, H., 2020. High-strength cellulose nanofibers produced via swelling pretreatment based on a choline chloride–imidazole deep eutectic solvent, *Green Chemistry*, 22, 1763–1775. https://doi.org/10.1039/C9GC04119B
[31] Guo, Y., Zhang, J., Wang, C., Liu, M., You, J., Yin, L., Shi, M., 2024. Green pretreatment of lignocellulosic biomasses via deep eutectic solvents, *Sustainable Chemistry and Pharmacy*, 39, 101569. https://doi.org/10.1016/j.scp.2024.101569

ARTICLE IN PRESS

[32] Mehdi Gholami, S., Koohestanian, E., 2025. Effective acetylation of hydroxyl compound with RuIII(OTf)2 Salen modified SiO2–Fe3O4 magnetically recycling catalyst, *Chemical Process Design*, 4, 38–49. https://doi.org/10.22111/cpd.2025.50678.1053
[33] Santana, I.K.C., Rocha, L.F., da S. Costa, B.G., Brito, J.F., Taube, P.S., Costa, J.A.S., de N. de Oliveira, A., Noronha, R.C.R., do Nascimento, L.A.S., Vasconcelos, A.A., 2026. The potential for obtaining nanostructured cellulose: An overview of current trends, *Processes*, 14, 2184. https://doi.org/10.3390/pr14132184
[34] Lim, J.J.Y., Hoo, D.Y., Tang, S.Y., Manickam, S., Yu, L.J., Tan, K.W., 2024. One-pot extraction of nanocellulose from raw durian husk fiber using carboxylic acid-based deep eutectic solvent with in situ ultrasound assistance, *Ultrasonics Sonochemistry*, 106, 106898. https://doi.org/10.1016/j.ultsonch.2024.106898
[35] Chyerochana, N., Huynh, Q.T., Jaitham, U., Phitsuwan, P., Aryusuk, K., Hongsibsong, S., Chen, K.-F., Chang, K.-L., 2025. Sustainable production of high-performance bioplastics from agricultural and industrial biomass waste by integrating deep eutectic solvent (DES) pretreatment and acetylation processes, *ACS Omega*, 10, 10949–10961. https://doi.org/10.1021/acsomega.4c09059
[36] Foster, E.J., Moon, R.J., Agarwal, U.P., Bortner, M.J., Bras, J., Camarero-Espinosa, S., Chan, K.J., Clift, M.J.D., Cranston, E.D., Eichhorn, S.J., Fox, D.M., Hamad, W.Y., Heux, L., Jean, B., Korey, M., Nieh, W., Ong, K.J., Reid, M.S., Renneckar, S., Roberts, R., Shatkin, J.A., Simonsen, J., Stinson-Bagby, K., Wanasekara, N., Youngblood, J., 2018. Current characterization methods for cellulose nanomaterials, *Chemical Society Reviews*, 47, 2609–2679. https://doi.org/10.1039/C6CS00895J
[37] Salem, K.S., Kasera, N.K., Rahman, M.A., Jameel, H., Habibi, Y., Eichhorn, S.J., French, A.D., Pal, L., Lucia, L.A., 2023. Comparison and assessment of methods for cellulose crystallinity determination, *Chemical Society Reviews*, 52, 6417–6446. https://doi.org/10.1039/D2CS00569G
[38] Lin, N., Dufresne, A., 2014. Nanocellulose in biomedicine: Current status and future prospect, *European Polymer Journal*, 59, 302–325. https://doi.org/10.1016/j.eurpolymj.2014.07.025
[39] Pradhan, D., Jaiswal, S., Tiwari, B.K., Jaiswal, A.K., 2024. Choline chloride–oxalic acid dihydrate deep eutectic solvent pretreatment of barley straw for production of cellulose nanofibers, *International Journal of Biological Macromolecules*, 281, 136213. https://doi.org/10.1016/j.ijbiomac.2024.136213

ARTICLE IN PRESS